Electronic Supplementary Material (ESI) for ChemComm.

Electronic Supplementary Information

Unraveling the Origin of Cooperative Adsorption of CO in Fe(II) Metal-Organic-Framework

Reshma Jose[a], Sourav Pal[b]*and Gopalan Rajaraman[a]*

Binding energy calculation

The binding energy (*BE*) for each CO binding is calculated using the following equations.

$$BE_1 = \frac{E_{MOF.nCo} - MOF_{Pristine(HS)} - E_{nCO}}{n} \qquad \text{(Eqn 1)}$$

BE_1 is the binding energy computed with respect to the high spin structure. Here $E_{MOF-nCO}$ is the optimized energy of the CO bound MOF where Fe bonund to CO has been kept in Low-spin state and unbound Fe were kept in high-spin state and $MOF_{Pristine(HS)}$ is the optimized energy of the unbound pristine MOF where all Fe atoms are in high spin state. E_{CO} is the optimized energy of CO molecule.

$$BE_2 = E_{MOF-nCO} - E_{MOF(n-1)CO} - E_{CO} \qquad \text{(Eqn 2)}$$

BE_2 is the computed binding energy of nth CO uptake with respect to the optimized geometry of the (n-1)th uptake. Here, $E_{MOF-nCO}$ correspond to the optimized energy of the nth CO bound MOF and $E_{MOF(n-1)CO}$ correspond to the optimized energy of the (n-1th) CO bound MOF and E_{CO} is the optimized energy of CO molecule. In all cases, the Fe bound to CO were kept in low-spin and the rest of unbound Fe atoms were in high-spin.

Cooperative Energy and Deformation Energy

The cooperative energy (*CE*) for successive binding is calculated based on the following equation.

$$CE = BE_1 - BE_2 \qquad \text{(Eqn 3)}$$

The deformation energy (*DE*) for successive binding is calculated based on the following equation.

$$DE_{nMOF} = (E_{nMOF-SP}) - (E_{pristine-MOF}) \qquad \text{(Eqn 4)}$$

Here DE_{nMOF} corresponds to the deformation energy of MOF for the nth uptake of CO. $E_{nMOF-SP}$ is the single point energy of the optimized structure of nth CO bound MOF after removing the n CO's. The Fe which is binding to CO are kept in low spin state for obtaining the single point energy. $E_{pristine-MOF}$ is the optimized energy of the high spin structure of unbound MOF.

$$DE_{CO} = (E_{CO-SP}) - (E_{CO-opt})$$

Here E_{CO-SP} is the energy of single point calculation performed on the optimized structure of CO bound MOF after removing the CO. Here E_{CO-opt} is the optimized energy of free CO.

Computational methodology

All calculations were carried out using periodic Density Functional Methods[1] using the PBE[2] functional incorporating dispersion effects as implemented in the CP2k suite. This methodology has proven to yield very good geometries for open-shell MOFs and has shown to yield a good numerical estimate of exchange coupling constants (*J*)[3, 4]. The Perdew−Burke−Ernzerhof (PBE)[5] gradient-corrected, generalized gradient approximation (GGA) was used to describe the exchange−correlation functional, and DZVP-MOLOPT-GTH (valence double zeta (ζ) plus polarization, molecularly optimized, Goedecker-Teter-Hutter) basis set for atoms (H, C, O, N, Cl) and DZVP-MOLOPT-SR-GTH for iron atom by incorporating the short-range forces with gaussian augmented plane wave (GAPW) approach with a kinetic energy cutoff of 400 Ry. The Grimme's D2 correction (DFT-D2) was used to account for the dispersion interactions. The entropy factor of CO molecule were taken from the NIST database. The entropy correction for CO (59 kJ/mol) were calculated using PBE functional with standard cc-pVDZ basis set. Our earlier studies have also shown a good estimate for geometries as well as exchange coupling costants based on the above explained computational methodology.[6, 7]

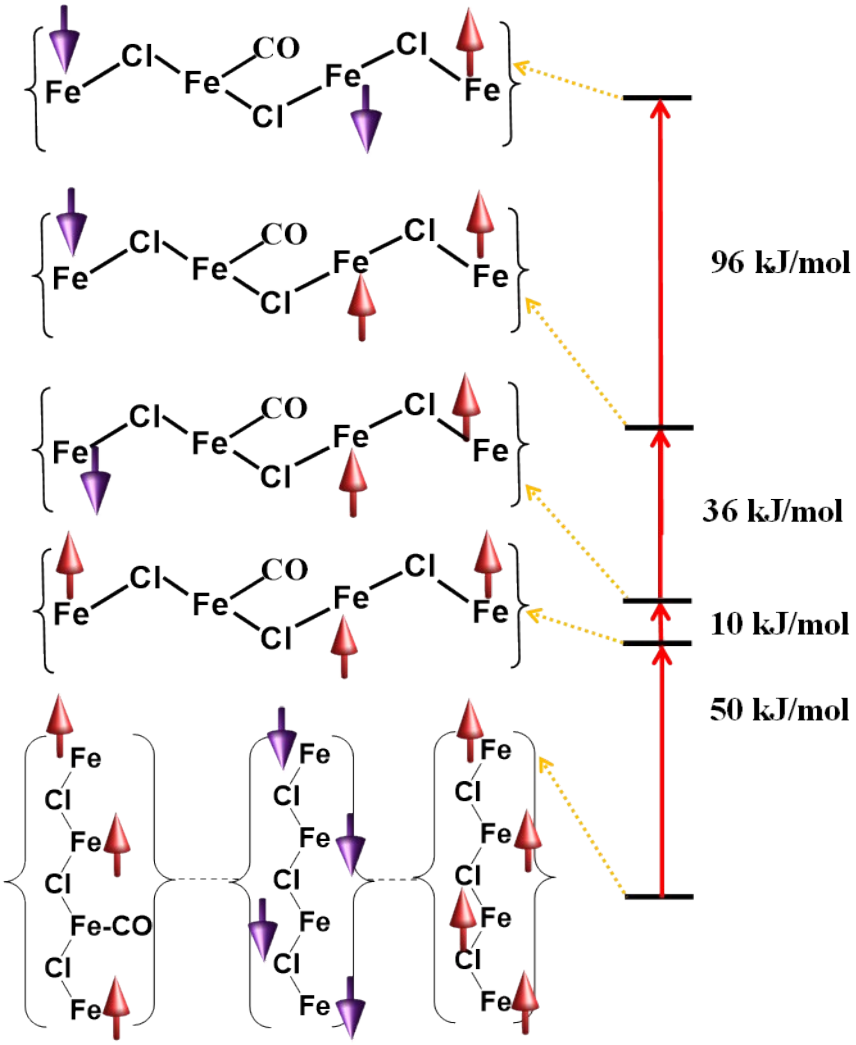

Figure S1: The various spin ladder and the energy difference between them noted in kJ/mol, for the CO bound **1**. Here Fe is in square octahedral geometry, and other coordinated atoms are omitted for clarity. The ground state and highest energy configuration have 196 kJ/mol energy differences. The high spin and ground-state configuration differ in 50 kJ/mol energy. The highest energy difference is between the antiferromagnetic spin-up-down-up-down configuration and ferromagnetic spin-down-up-up configuration within a tetrameric unit.

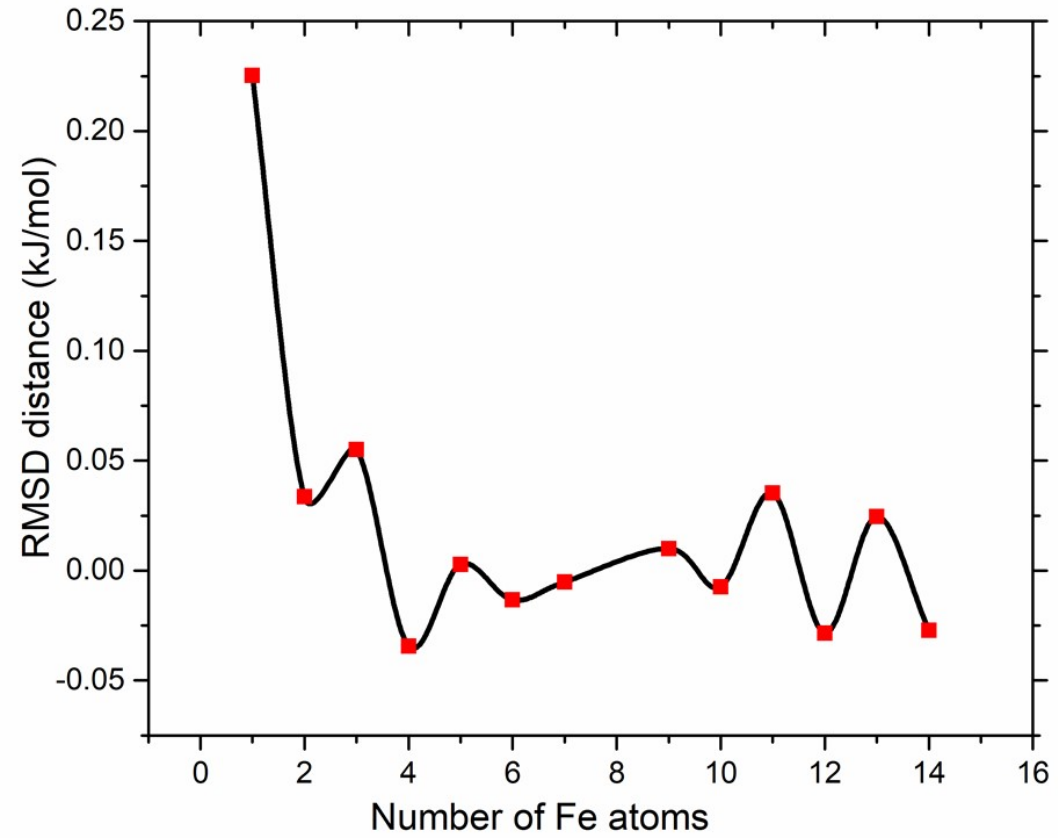

Figure S2: The plot of root mean square deviation in bond distances (Å) for the 1CO bound Fe MOF with respect to the unbound MOF.

$$RMSD = \sqrt{\sum_{n=1\ to\ 24} ((Fe_n - N_1)_{pristine-HS} - (Fe_n - N_1)_{bound-LS}))^2 + ((Fe_n - N_2)_{bound-LS}))^2 + + ((Fe_n - Cl)_{pristine-HS} - (Fe_n - Cl)_{boun}}$$

Here n=1,2,3…24. Fe-N_1 is the average axial Fe-N distance and Fe-N_2 is the average terminal Fe-N distance.

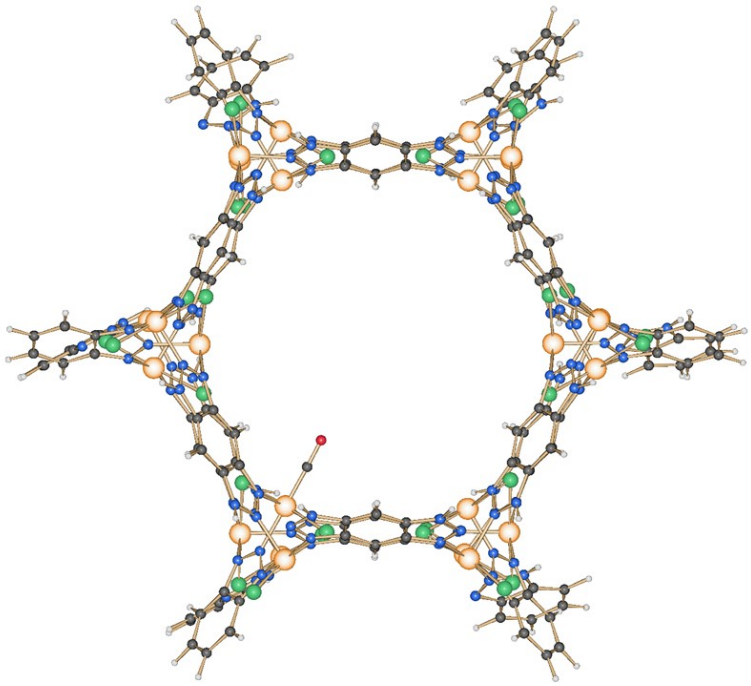

Figure S3: The structure of the 1CO bound MOF, reoptimized from the final geometry of 2CO bound MOF. The estimated binding energy (-74.2 kJ/mol) which is slightly higher than the direct binding case of 1st CO, which is -60.1 kJ/mol. Here average Fe-Cl, Fe-N, Fe-CO bond distances are 2.29Å, 1.97 Å, 1.72 Å, respectively.

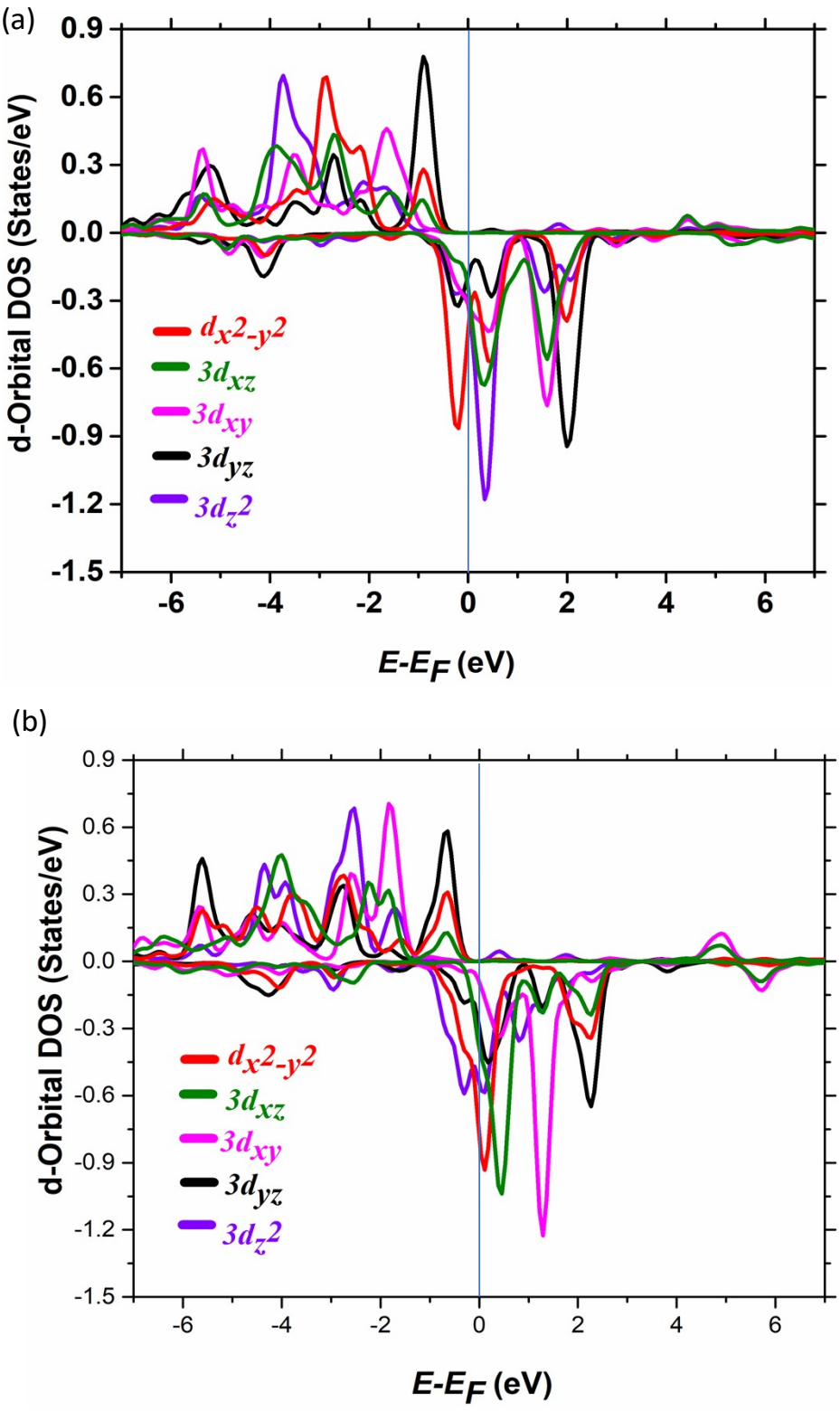

Figure S4: The Partial density of state plot for (a) nearest neighboring Fe centre of Fe1 in the unbound state (b) CO bound state.

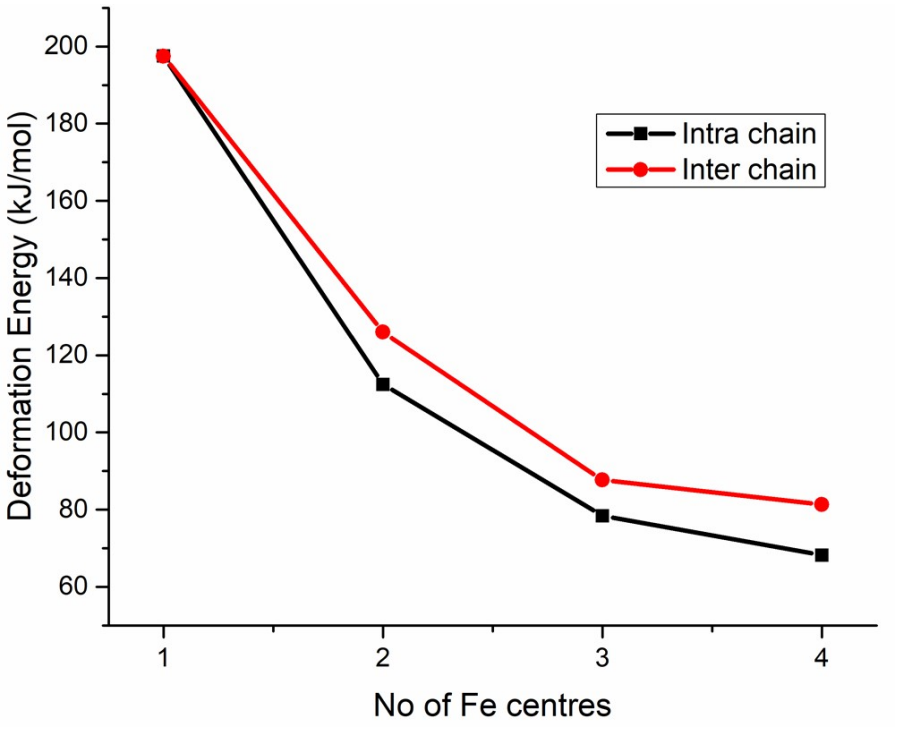

Figure S5: The trend in deformation Energy along z- axis and along x axis (inter chain).

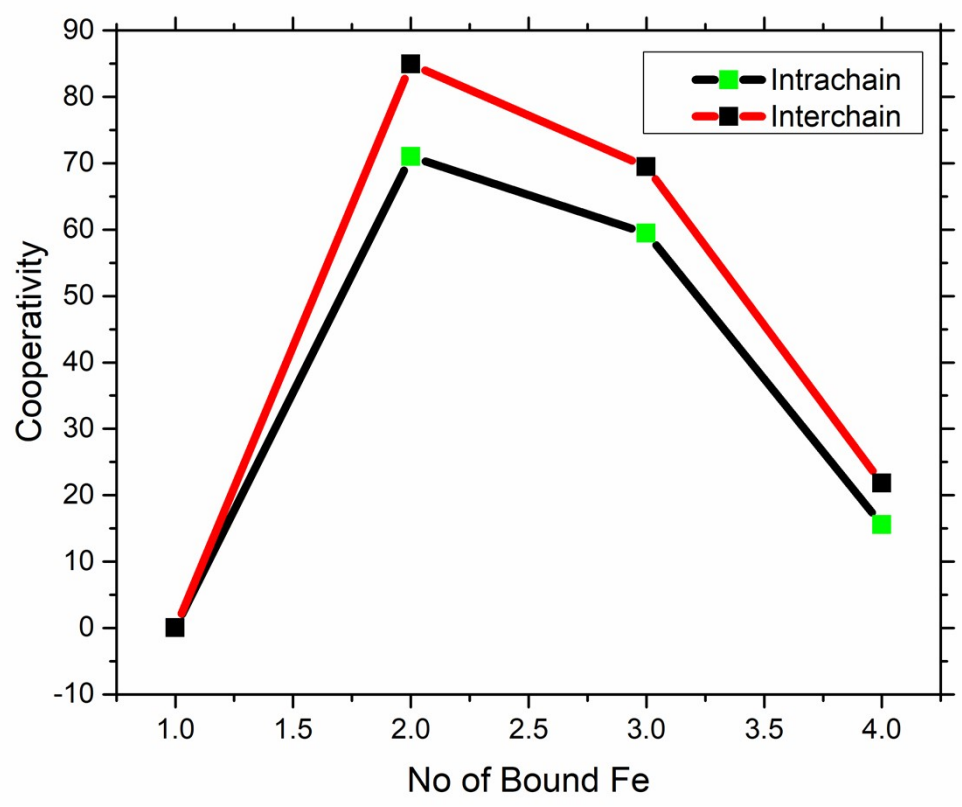

Figure S6: The trend in intra and inter-chain cooperativity (in kJ/mol) for the addition of up to 4 COs.

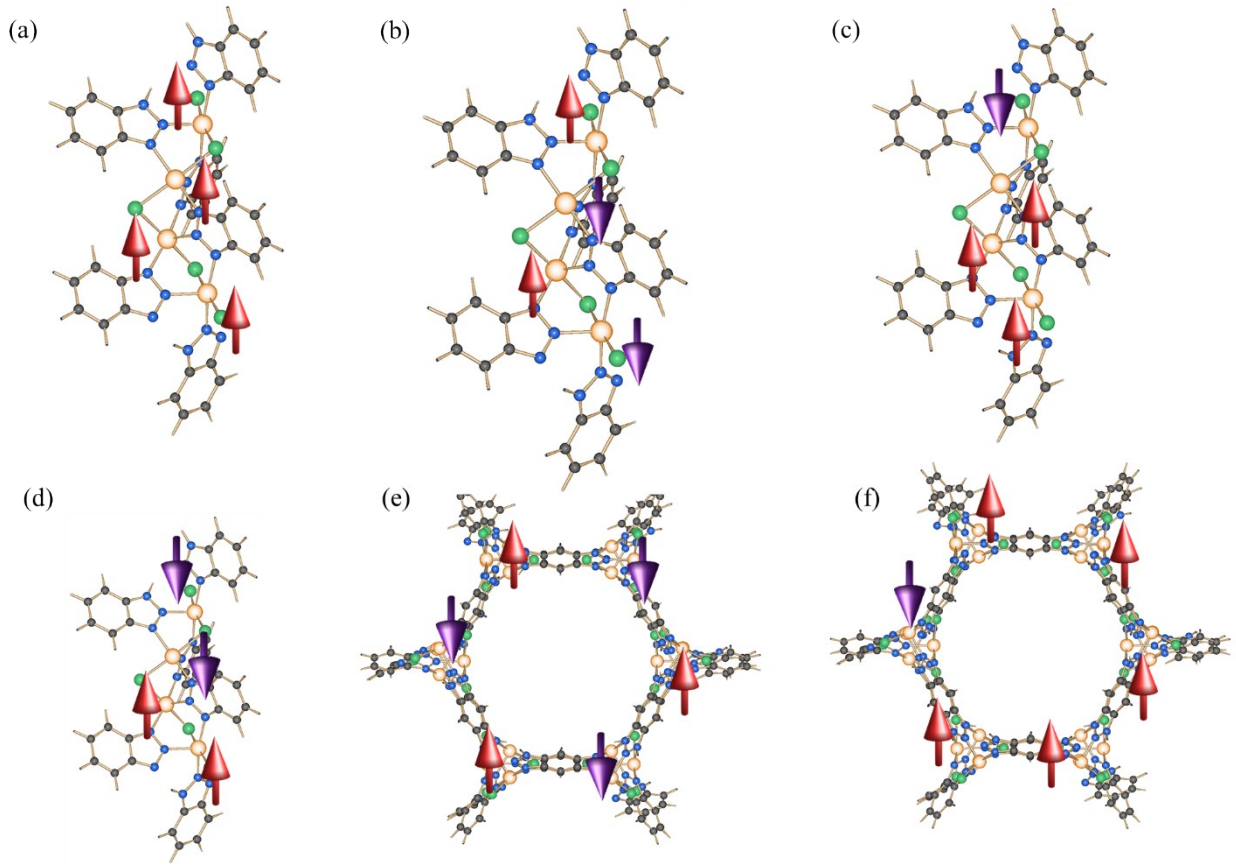

Figure S7. The broken symmetry configuration considered for the magnetic coupling. (a) HS, (b) BS1, (c) BS2, (d) BS3, (e) BS4, (f) BS5

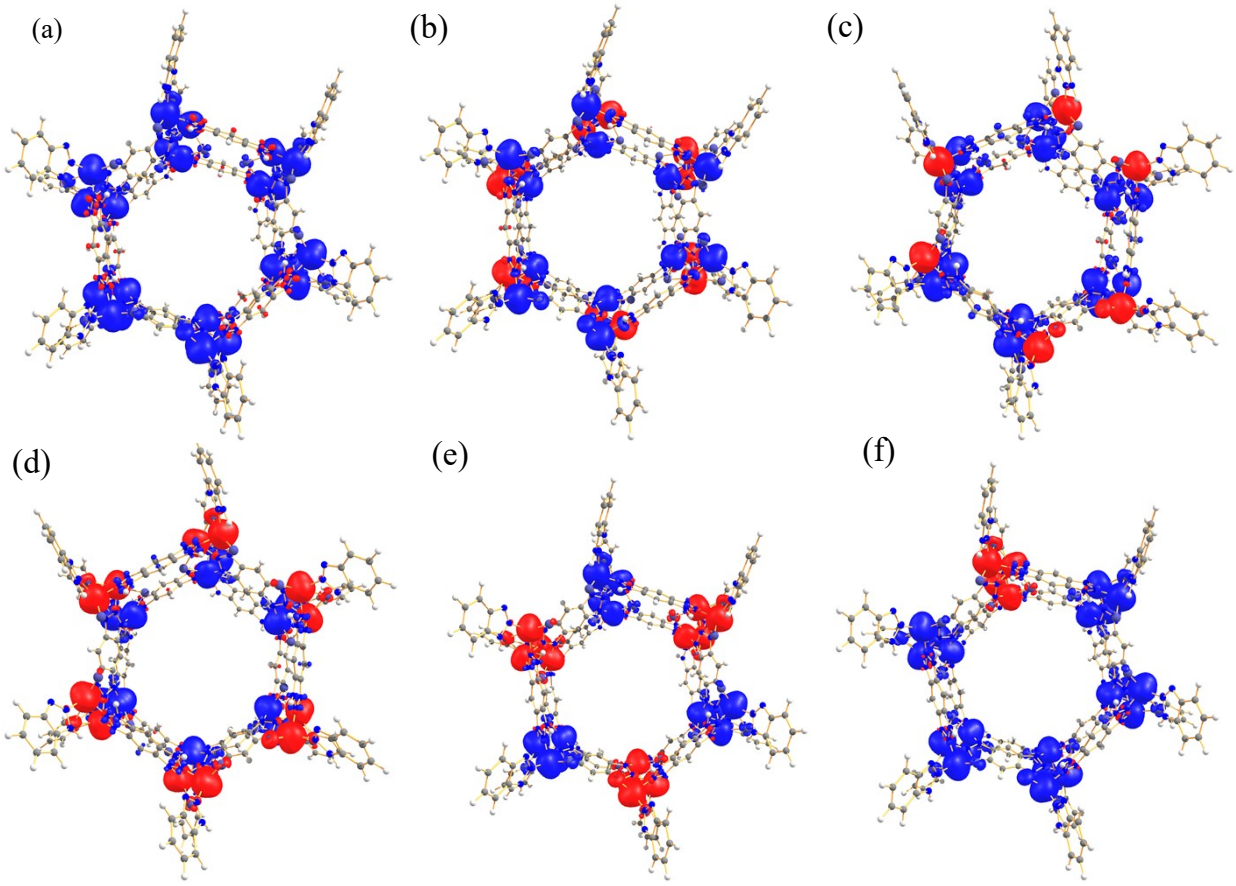

Figure S8: The spin density plot of each spin configurations with a cut off value of 0.008 a.u. (a) HS, (b) BS1, (c) BS2, (d) BS3, (e) BS4, (f) BS5

The small tetrameric model system, repeats in the z-axis, explains the spin configurations (a) to (d), where each tetrameric unit had the same alignment of spins. BS1 contains nearby iron centers as spin-up-down-up-down configuration. The BS2 has only one iron in down spin, and the other three are in up spin configurations. The BS3 contains two nearby iron centers with a spin configuration as up-up -down-down. The BS4 and BS5 configurations were chosen to understand the exchange between adjacent tetrameric units. In the BS4 configuration, each alternate tetramer was set to either spin up or spin down orientation. The BS5 has only one tetramer in down spin configuration, and other units were in high spin. All these broken symmetries were taken for the calculations and obtained the energy of each of them. The spin density diagram corresponding to each broken symmetry is shown in figure 6.4. A cut-off energy of 0.008 a.u. for obtaining the spin density diagrams. The blue color shows the alpha spin density, and the red color indicates the beta spin density. The maroon color arrow indicates the total positive spin density at each tetrameric iron site. The purple color arrow indicates the negative spin density around each tetrameric iron site.

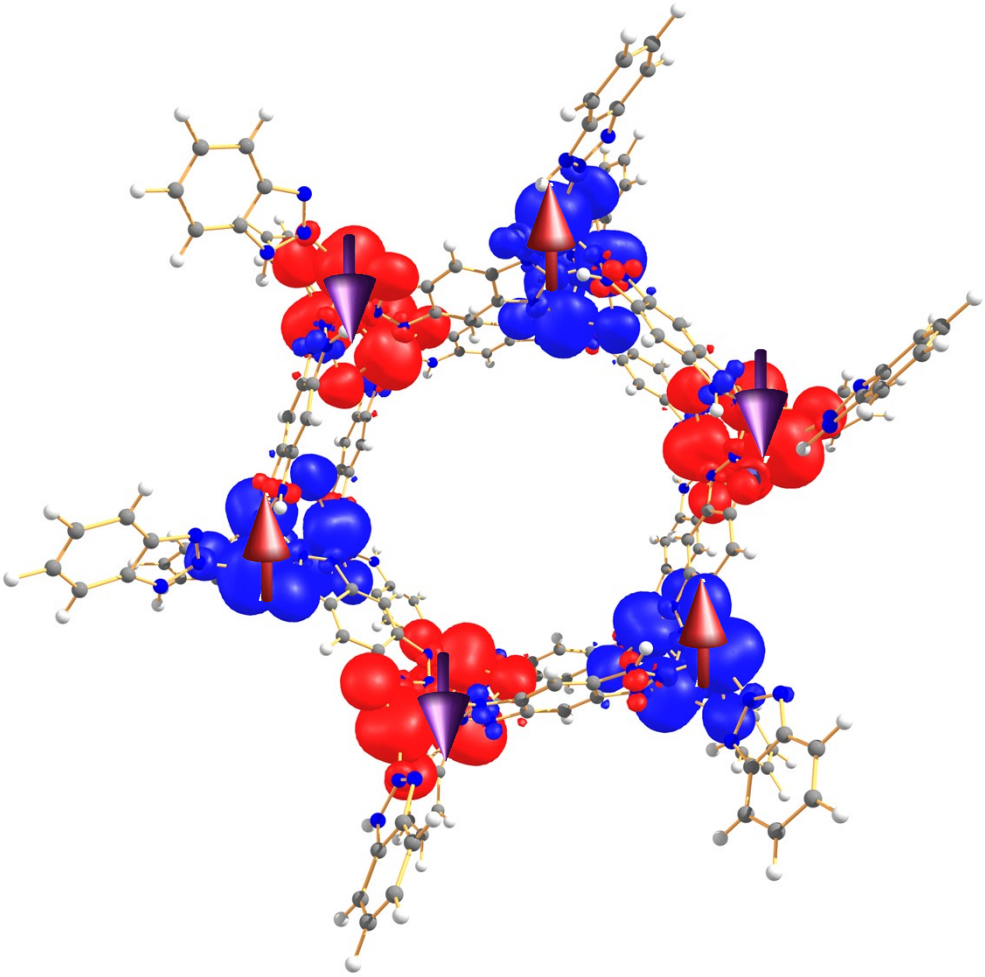

Figure S9: The ground state spin configuration of Fe-MOF among the computed broken symmetry configurations, at a spin density cut off value of 0.008 a.u.

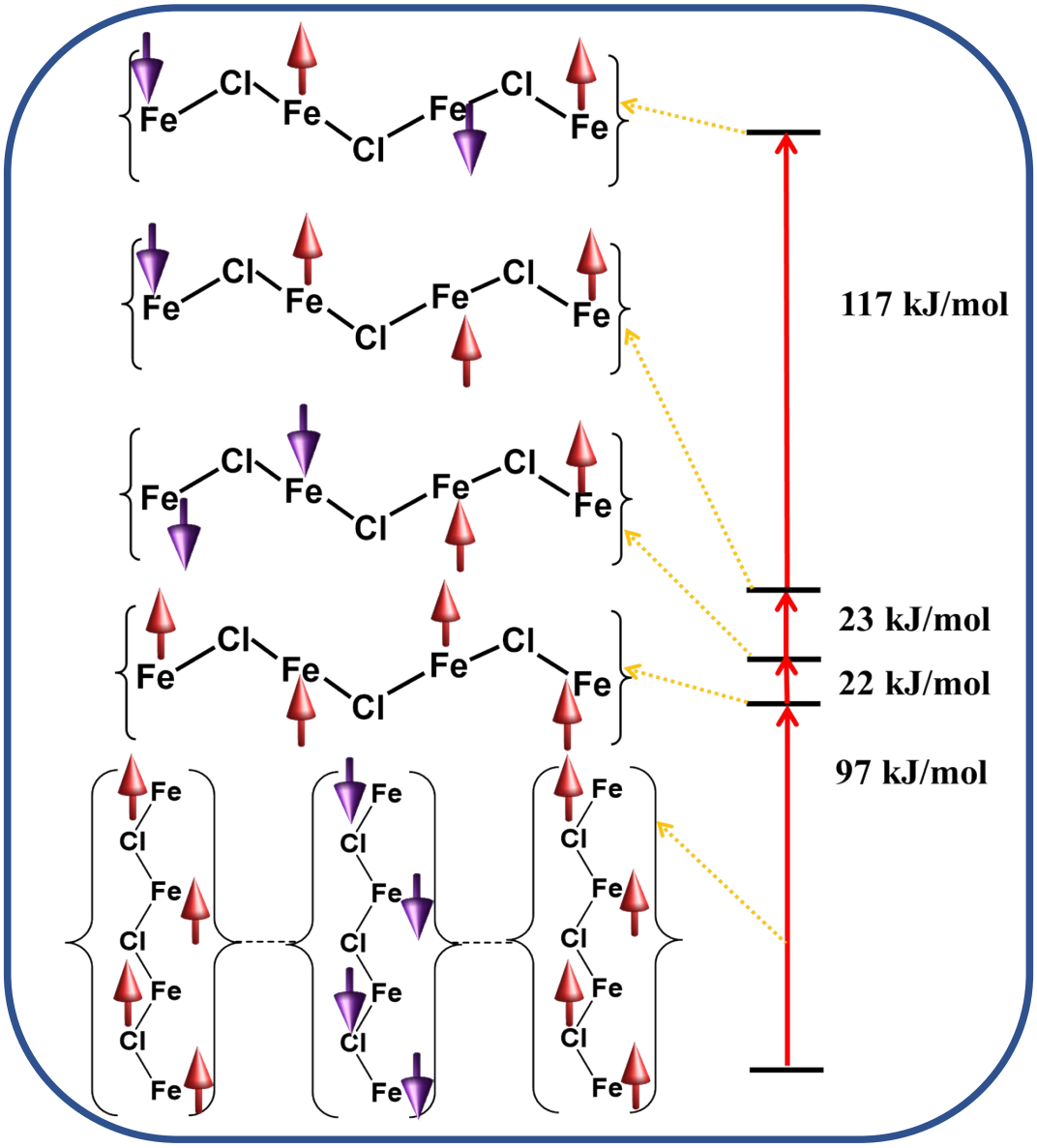

Figure S10. The various spin ladder for **1** and before binding of CO, the energy difference between them (kJ/mol). Here Fe is in square pyramidal geometry, and other coordinated atoms are omitted

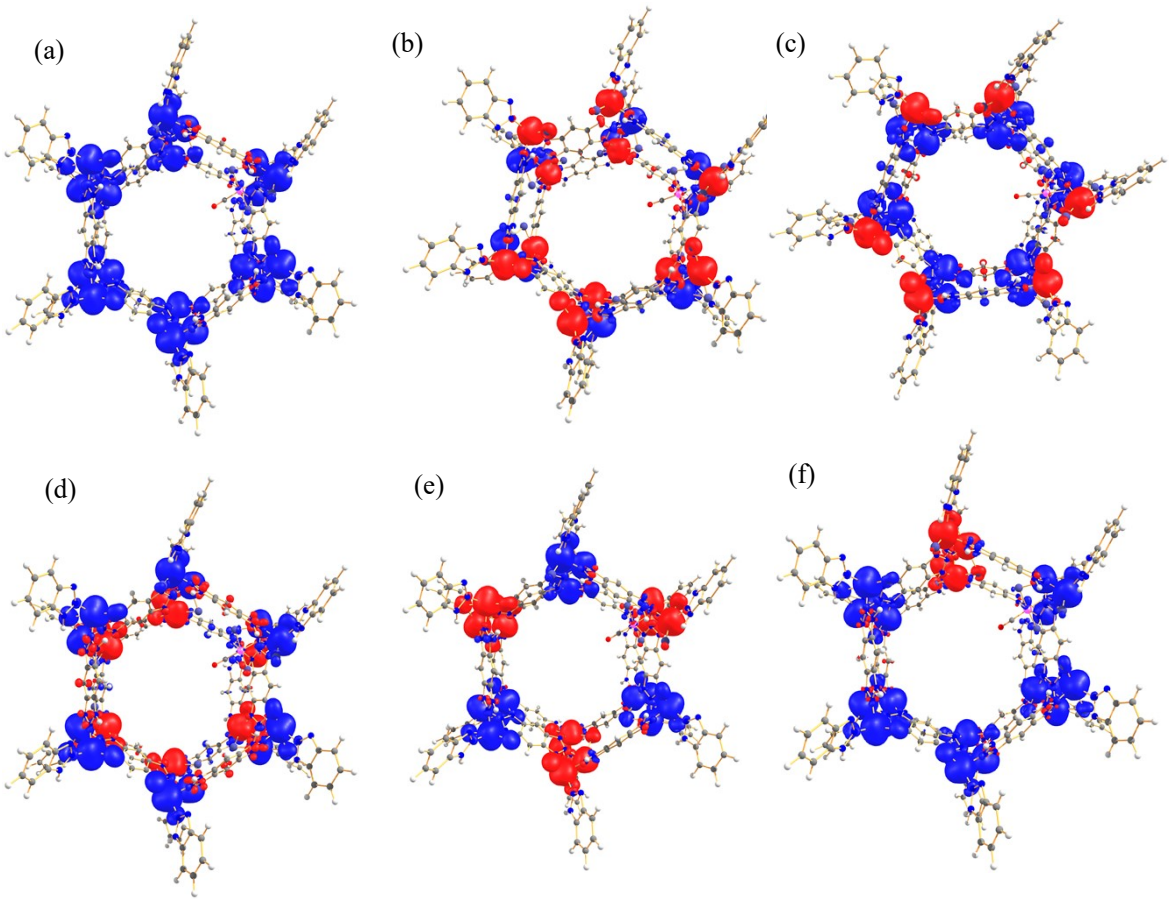

Figure S11: The spin density plot of each spin configurations after CO binding, with a cut off value of 0.008 a.u. (a) HS, (b) BS1, (c) BS2, (d) BS3, (e) BS4, (f) BS5

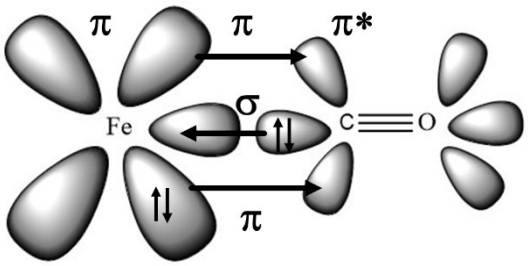

Figure S12: The chemdraw diagram depicting the Fe and CO bonding and back bonding synergic interactions.

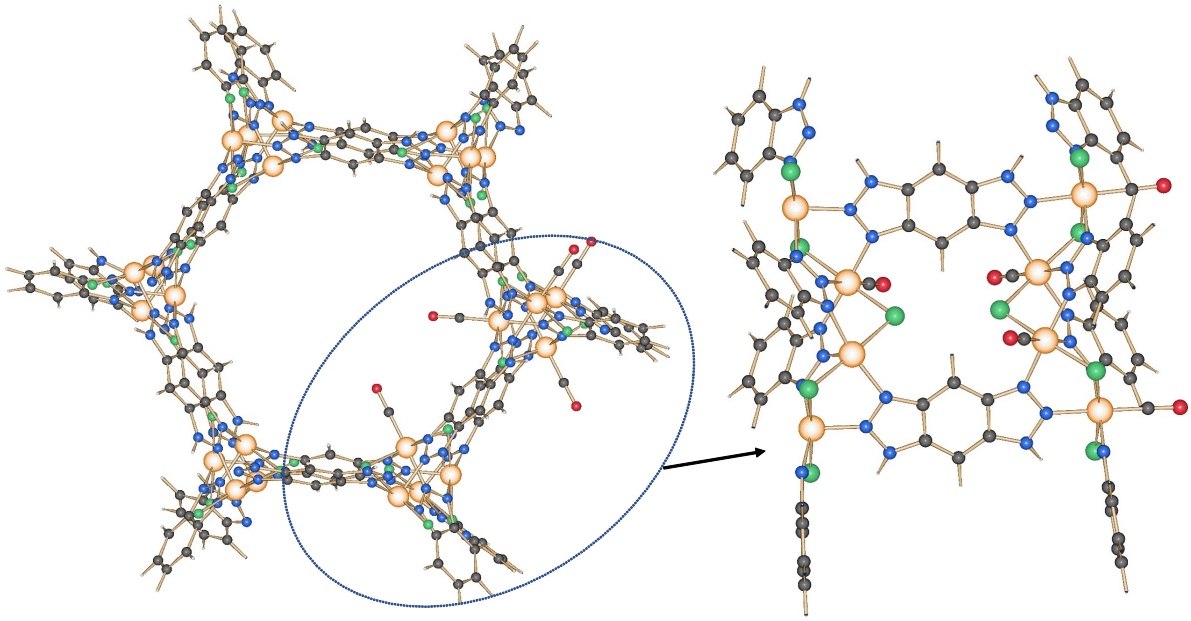

Figure S13: The structure of the 5CO bound form and its enlarged view

Table S1. The changes in structural parameters of unbound MOF during successive binding of CO

Binding of n^{th} CO	Bond parameters	Average Fe-N (Å)	Fe-Cl (Å)	Fe-Cl-Fe (°)
1^{st} CO	Unbound-Fe	2.021	2.413	85
	Fe_1	1.973	2.293	92.3
	Fe_2	2.06	2.27	93.7
	Unbound	2.021	2.413	85.0
2^{nd} CO	Fe_1	1.959	2.293	93.0
	Fe_2	1.970	2.271	96.0
	Fe_3	2.030	2.360	91.8
	Unbound	2.021	2.413	85.10
3^{rd} CO	Fe_1	1.934	2.277	95.57
	Fe_2	1.969	2.270	96.09
	Fe_3	1.972	2.277	93.07
	Unbound	2.021	2.413	85.10
4^{th} CO	Fe_1	1.945	2.279	95.31
	Fe_2	1.974	2.268	96.44

	Fe_3	1.958	2.271	96.75
	Fe_4	1.972	2.286	96.75
	Unbound	2.021	2.413	85.10
5^{th} CO	Fe_1	1.932	2.269	96.27
	Fe_2	1.939	2.265	96.64
	Fe_3	1.928	2.254	96.93
	Fe_4	1.923	2.276	96.93
	Fe_5	1.983	2.305	92.37
	Unbound	2.021	2.413	85.10
6^{th} CO	Fe_1	1.937	2.267	95.97
	Fe_2	1.939	2.272	96.67
	Fe_3	1.928	2.254	96.93
	Fe_4	1.932	2.280	96.48
	Fe_5	1.936	2.275	96.71
	Fe_6	1.961	2.287	91.79

Table S2: The Successive CO binding and trend in deformation energy and cooperative energy

No of bound CO	BE_1(kJ/mol) (Without entropy factor)	BE_2(kJ/mol) (Without entropy factor)	*DE* (kJ/mol) (Intra chain)	*DE* (kJ/mol) (Inter chain)	*CE* (kJ/mol) (Intra chain)	*CE* (kJ/mol) (Inter chain)
1CO	-119.05	-119.05	197.5	197.5	0	0
2CO	-203.95	-288.87	112.42	126.0	84.9	70.9
3CO	-238.71	-308.18	78.4	87.7	69.5	59.5
4CO	-245.97	-267.76	68.2	81.3	21.8	15.6
5CO	-254.12	-285.95	61.8	-	31.8	-

Table S3: The binding energy comparison CO with respect to H_2 and N_2 (values in kJ/mol).

n^{th} CO uptake	BE_{CO}	BE_{H2}	BE_{N2}
1	-60.1	-18.78	-37.08
2	-145.0	-16.36	-41.91
3	-179.7	-17.87	-31.11
4	-187.0	-18.59	-30.15

Table S4. The structural parameters of bound CO upon successive addition.

Bond parameters		Fe-C (Å)	C-O (Å)	Fe-C-O (°)
1^{st} CO	Fe_1	1.732	1.158	178.8
2^{nd} CO	Fe_1	1.730	1.157	177.58
	Fe_2	1.740	1.163	178.40
3^{rd} CO	Fe_1	1.719	1.168	178.53
	Fe_2	1.733	1.165	177.61
	Fe_3	1.746	1.158	174.33
4^{th} CO	Fe_1	1.722	1.161	177.81
	Fe_2	1.738	1.159	178.05
	Fe_3	1.743	1.167	173.69
	Fe_4	1.750	1.165	178.42
5^{th} CO	Fe_1	1.731	1.163	178.37
	Fe_2	1.721	1.163	179.25
	Fe_3	1.734	1.164	178.78
	Fe_4	1.743	1.162	178.95
	Fe_5	1.732	1.163	179.26
6^{th} CO	Fe_1	1.726	1.166	179.52
	Fe_2	1.724	1.163	178.14
	Fe_3	1.731	1.167	178.86
	Fe_4	1.734	1.161	178.84
	Fe_5	1.732	1.163	179.75
	Fe_6	1.173	1.166	178.58

Table S5: The bond parameters taken for RMSD plot (figure S1), here Fe_n-HS corresponds to bond parameters of each iron centre in high spin before binding of CO. The Fe_n-1CO represents the bond parameters of each iron centre after 1CO is bound.

Bond Parameters	Axial Fe-N	Terminal Fe-N_1	Terminal Fe-N_2	Bridging Fe-Cl	Bridging Fe-Cl_2
Fe1-HS	1.97583	2.00834	2.04566	2.39399	2.44242
Fe1-1CO	2.00153	1.95401	1.95793	2.28508	2.30297
Fe2-HS	1.97051	2.05154	2.18348	2.24707	2.36962
Fe2-1CO	1.98471	2.06529	2.14883	2.22007	2.36613
Fe3-HS	1.98225	2.09887	2.0316	2.28198	2.42165
Fe3-1CO	1.98654	2.05566	2.03855	2.25882	2.44658
Fe4-HS	1.99513	1.99484	2.06272	2.24207	2.53424
Fe4-1CO	1.98102	2.00745	2.0968	2.2438	2.54125
Fe5-HS	1.97300	2.04206	2.16588	2.38676	2.25865
Fe5-1CO	1.97366	2.05077	2.16308	2.37741	2.25503
Fe6-HS	1.97569	2.02564	2.06827	2.37587	2.41746
Fe6-1CO	1.97869	2.01654	2.06736	2.3962	2.43706
Fe7-HS	1.98248	2.09333	2.03444	2.26665	2.43536

Fe7-1CO	1.98251	2.11329	2.04366	2.28401	2.41138
Fe8-HS	2.00072	1.96774	2.03504	2.22395	2.67239
Fe8-1CO	2.00521	1.97851	2.06184	2.24202	2.56156
Fe9-HS	1.96920	2.01078	2.0821	2.44027	2.31088
Fe9-1CO	1.96455	2.00425	2.08791	2.43562	2.31058
Fe10-HS	1.97077	2.09817	2.03825	2.38497	2.38459
Fe10-1CO	1.96152	2.11693	2.04995	2.37108	2.39378
Fe11-HS	1.97662	2.07172	2.02213	2.44977	2.29588
Fe11-1CO	1.97543	2.04689	2.00280	2.48436	2.30603
Fe12-HS	1.99628	2.01556	2.07707	2.23003	2.50915
Fe12-1CO	1.99236	2.0131	2.10149	2.24046	2.49421
Fe13-1CO	1.97504	2.02551	2.10799	2.42211	2.28304
Fe13-HS	1.97578	2.00984	2.08800	2.45213	2.29334
Fe14-HS	1.97292	2.02424	2.07993	2.37263	2.39652
Fe14-CO	1.96246	2.04604	2.108800	2.37745	2.38345
Fe15-HS	1.96844	2.00900	2.010770	2.44873	2.39338
Fe15-1CO	1.97201	2.04055	2.001090	2.44824	2.32107
Fe16-HS	2.01764	2.04776	2.093700	2.42294	2.19818
Fe16-1CO	1.99296	2.08400	2.007590	2.49713	2.20090

References

1. D. Nazarian, P. Ganesh and D. S. Sholl, *J. Mater. Chem. A*, 2015, **3**, 22432-22440.
2. J. Paier, R. Hirschl, M. Marsman and G. Kresse, *J. chem. phys.*, 2005, **122**, 234102.
3. S. Schwalbe, K. Trepte, G. Seifert and J. Kortus, *Phys. Chem. Chem. Phys.*, 2016, **18**, 8075-8080.
4. S. O. Odoh, C. J. Cramer, D. G. Truhlar and L. Gagliardi, *Chem. Rev.*, 2015, **115**, 6051-6111.
5. J. N. Harvey, *Annu. Rep. Prog. Chem., Sect. C: Phys. Chem.*, 2006, **102**, 203-226.

6. R. Jose, S. Pal and G. Rajaraman, *Chem.Phys.Chem*, 2023, **24**, e202200257.
7. R. Jose, S. Kancharlapalli, T. K. Ghanty, S. Pal and G. Rajaraman, *Chem. Eur. J.*, 2022, e202104526.